Available online at www.pelagiaresearchlibrary.com

Pelagia Research Library

Der Chemica Sinica, 2018, 9(3):750-761

ISSN : 0976-8505
CODEN (USA): CSHIA5

Binding Energy of Methane with Metal Dication Complex Ion [Mn(BENZENE)2]2+ in the Gas Phase

Joseph K Koka[1,2*]

[1]*School of Chemistry, University of Nottingham, University Park, Nottingham NG7 2RD, United Kingdom*
[2]*School of Physical Science, Department of Chemistry, University of Cape Coast, Ghana*

ABSTRACT

A theoretical and experimental study on $[Mn(Benzene)_2]^{2+}$ has been undertaken in the gas phase. The ions were prepared using a combination of the pick-up technique and high energy electron impact, and then held in a cold ion trap where they were excited with tuneable UV radiation and further activated with methane. The following $[Mn(Benzene)2\ CH_4]^{2+}$, $[Mn(Benzene)2(CH_4)_2]+$, $[Mn(Benzene)2(CH_4)2H_2O)]+$ and $[Mn(Benzene)2CO_2(CH_3)_2]+$ were successfully identified after the experimental analysis. Two optimised geometries of $[Mn(Benzene)_2]^{2+}$ were observed, namely the C2V eclipse and C2 staggered .

The DFT calculated binding energy of methane to manganese benzene dication complex ion $[Mn(Benzene)_2]^{2+}$ at BP86/6- 311++G(d, p) is 15.30 kJ/mol comparing with the calculated 20.55 kJ/mol recorded on the potential energy curve (PEC). The difference of about 5.25 kJ/mol results from the fact that the calculated charge on the manganese metal centre at the optimised geometry of $[Mn(Benzene)2\ CH_4]_2+$ was 1.30 while a charge of Mn=2.0 was assumed in the PEC calculation.

Keywords: Binding energy, Methane, Manganese, Benzene, Dication.

INTRODUCTION

Gas phase chemistry of ions provides important insight into the reactivity, thermochemistry, reaction mechanisms, and structures of ions without the added complexity of solvent. Although a lot of work has been done both theoretically and experimentally on metal-benzene complexes very little if not at all is focused on activation of methane with manganese-benzene complexes. Literature revealed that Soteras et al. has theoretically investigated the structural and electronic effects of the interaction of six singly charged metal cations including manganese with benzene [1]. Kurikawa et al. in the gas-phase produced, neutral metal−benzene complexes, $M_n(benzene)_m$ (M = Sc to Cu), using a laser vaporization method and characterized them by mass spectrometry, photoionization spectroscopy, and chemical probe experiments [2].The neutral (M_nBz_{n+1}) was studied by Miyajima et al. using magnetic deflection approach including vanadium−benzene organometallic complexes $Vn(C_6H_6)m$ produced by a laser vaporization synthesis method.

Xiang et al theoretical studied the electronic and magnetic properties for MBz polymers with M=Sc, Ti, V, Cr, and Mn has shown that all chains, except CrBz are metallic [3] Martínez et al. in their work presented first-principles calculations of the photoabsorption cross sections of M_nBz_{n+1} sandwiches with M=Ti, V, Cr, and $n \leq 3$ [4,5]. While Ravindra et al. studied the electronic Structure and Properties of Transition Metal-Benzene Complexes and observed that the variation of the metal−benzene distances, dissociation energies, ionization potentials, electron affinities, and spin multiplicities across the 3D series in MBz complexes differs qualitatively from those in $M(Bz)_2$ [6]. Again, Miyajima et al. by a laser vaporization synthesis method produced metal−benzene organometallic clusters $M_n(C_6H_6)_m$ (M =Al, Sc, Ti, and V) [7]. Willey et al. using laser vaporization investigated photo dissociation dynamics, spectroscopy and binding energies of metal ion-benzene complexes [8]. Meyer et al. by collision–induced dissociation with Xe guided beam tandem mass spectrometer determined the sequential bond energies of the mono–bis benzene complexes of the first row transition metal ions $M^+ = Ti^+$-Cu^+[9]. Binding energies were successfully estimated for the complexes

of benzene with the first-row transition-metal ions ($M^+ = Ti^+ - Cu^+$) *via* both kinetic modeling and quantum chemical simulation [10]. Hongming et al. using maximally localized wannier functions analysed details of closely related materials, single benzene (Bz) molecule, organometallic vanadium-Bz infinite chain, and V_2Bz_3 sandwich cluster [11]. Jaeger et al. by the application of laser vaporization produced $Ni^+(benzene)_n$ (n=1−6) and $Ni^+(benzene)_n$ (n=1,2) [12] and further produced metal-benzene complexes of the form M(benzene)n (M = Ti, V, Fe, Co, Ni) [13-17].

Despite the fact that carbon dioxide is typically painted as the bad boy of greenhouse gases and its emissions are five times greater than methane, they are similarly problematic because methane is roughly 25 times the global warming potential of carbon dioxide [18]. Recent calculations suggest that atmospheric CH_4 emissions have been responsible for approximately 20% of Earth's warming since pre-industrial times [19]. Hence any large-scale chemical conversion of methane into other valuable and/or environmentally friendly chemical compounds would have a remarkable impact on the climate. Bis benzene manganese dication complex ions $[Mn(Benzene)_2]^{2+}$ were formed in the gas phase and activated with methane. The binding energies of methane to the metal complexes were calculated. Once methane is activated it can serve as feedstock formation in a vast variety of important industrial reactions. Imagine a small plant that has methane as input where resources of methane could be used much more efficiently. For instance steam reforming converts methane into syngas, Equation (1), from which methanol can be produced in a second step [Equation (2)], or partial oxidation of methane according to Equation (3) to produce methanol as a liquid.

$CH_4 + H_2O \rightarrow CO + 3H_2$ Equation 1

$CO + 2H_2 \rightarrow CH_3OH$ Equation 2

$CH_4 + O_2 \rightarrow CH_3OH$ Equation 3

EXPERIMENTAL

MATERIALS AND METHODS

Manganese, Benzene, helium buffer gas, liquid nitrogen, ion trap, Nd:YAG-pumped dye laser, oscilloscope

Experimental section

$[Mn(Benzene)_2]^{2+}$ ions were synthesised in the gas phase and their spectra recorded *via* UV photofragment spectroscopy within an ion trap mass spectrometer cooled to between 100-150 K. A schematic diagram of the apparatus is shown in **Figure 1**. Neutral $Mn[Benzene]_n$ clusters were generated *via* the pickup technique [20], whereby argon carrier gas at a pressure of 130 psi was passed through a reservoir of benzene held at room temperature. The resultant mixture, containing approximately 1% benzene vapour, underwent supersonic expansion through a 50 mm diameter nozzle before passing through a 1 mm diameter skimmer.

The emerging beam of mixed argon/pyridine clusters then passed over the top of a Knudsen cell containing manganese chips heated to 1150°C, which was sufficient to generate a metal vapour pressure of 10^{-3} to 10^{-2} mbar. Collisions between metal vapour and the mixed clusters generated neutral metal-containing clusters, which were then ionised by

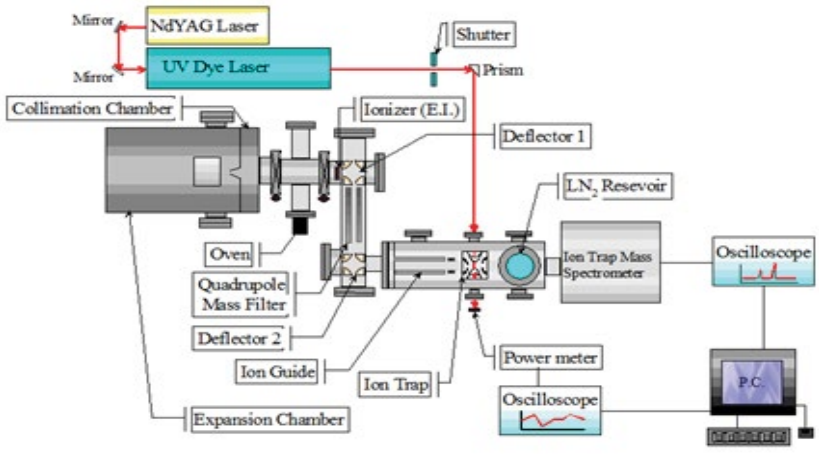

Figure 1: The diagram illustrating the experimental set up.

high energy electron impact (100 eV) in the ion source of a quadrupole mass spectrometer (Extrel). From the mixture a doubly charged ions, $[Mn(Benzene)_2]^{2+}$ was mass selected and directed by an ion guide into a Paul ion trap. The end caps of the latter were grounded and continuously cooled through direct contact with a liquid nitrogen reservoir. As a result, helium buffer gas (5×10^{-4} mbar) contained within the trap was also cooled and over a total trapping time of 1s, collisions between the helium and trapped ions led to a considerable reduction in the internal energy content of the latter [21]. Based on the observation of unimolecular decay by trapped ions, the internal temperature was thought to drop from 4500 K to somewhere in the range 100–150 K [22]. This cooling procedure has led to the appearance of discrete structure in the spectra (**Figure 2**).

RESULTS AND DISCUSSION

Following a 300 ms collection and cooling period, the ions were irradiated with seven 10 ns pulses of tunable UV radiation from the frequency-doubled output of a Nd: YAG-pumped dye laser, before being ejected for mass analysis and signal averaging. This gave a total duty cycle of 1 s for each period of ion injection and excitation. Photon absorption led to fragmentation, and the intensities of the precursor and all fragment ions were monitored as a function of photon energy. The cycle of trapping and laser excitation was repeated 200 times to yield a photofragment mass. **Figure 3** revealed UV photofragment mass spectrum of $[Mn(Benzene)_2]^{2+}$ complex ion with four distinct peaks with the dication complex ion demonstrated the ability to coordinate with water to form the hydrated photofragment $[Mn(Benzene)_2\ H_2O]^{2+}$ at 114.5 amu. The photofragmentation pattern is the loss of benzene and the formation of $BenzeneH^+$ fragment at 79 amu a clear evidence of charge transfer process between the manganese and the benzene permitting the complex to abstract a proton from the water or benzene molecule. The ability of benzene molecule to further photofragment to form $C_4H_4^+$ ion peak at 52 amu was recorded with another peak at 55 amu corresponding to Mn^+ and the total fragment signal was counted as the sum of intensities of these peaks.

Photofragmentation of $[Mn(BENZENE)_2]^{2+}$

A proposal for the two possible routes of photoexcitation of trapped $[Mn(Benzene)_2]^{2+}$ can as follows:

Mechanism 1: $[Mn\ (Benzene)_2]^{2+} + h\nu \rightarrow [Mn\ (Benzene)\ ]^+ + Benzene^+$

$[Mn\ (Benzene)]^+ + h\nu \rightarrow Mn + Benzene^+$

$Benzene^+ + h\nu \rightarrow C_4H_4^+ + C_2H_2$

Mechanism 2: $[Mn\ (Benzene)_2]^{2+} + h\nu \rightarrow [Mn\ (Benzene)]^{2+} + Benzene$

$[Mn\ (Benzene)]^{2+} \rightarrow Mn^+ + Benzene^+$

$Benzene^+ + h\nu \rightarrow C_4H_4^+ + C_2H_2$

From the ionisation energy point of view the first ionization energies of manganese and Benzene [IE (Mn) =7.43 eV, IE (Bz) = 9.24 eV] are both lower than the second ionization energy of manganese (2^{nd} IE (Mn) = 15.64 eV), an indication that Mn^+ and $benzene^+$ should be produced rather than Mn^{2+} and neutral benzene. Due to the charge

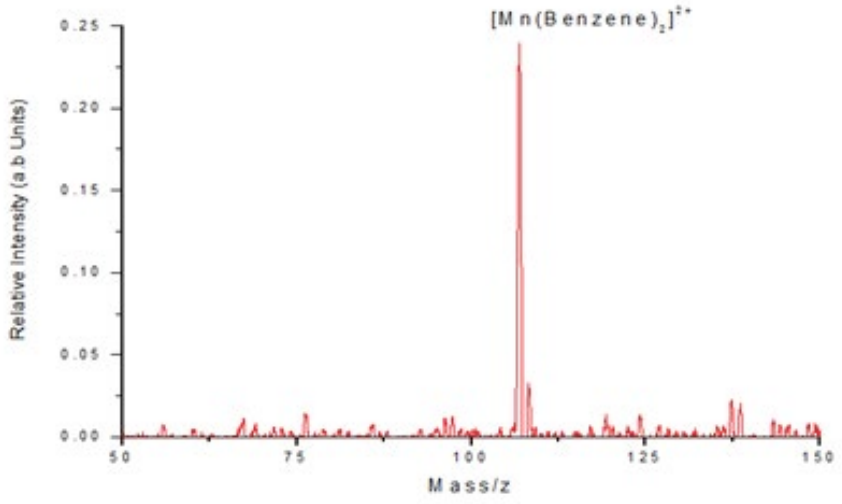

Figure 2: Mass spectrum of manganese benzene dication complex ion. $[Mn(Benzene)_2]^{2+}$.

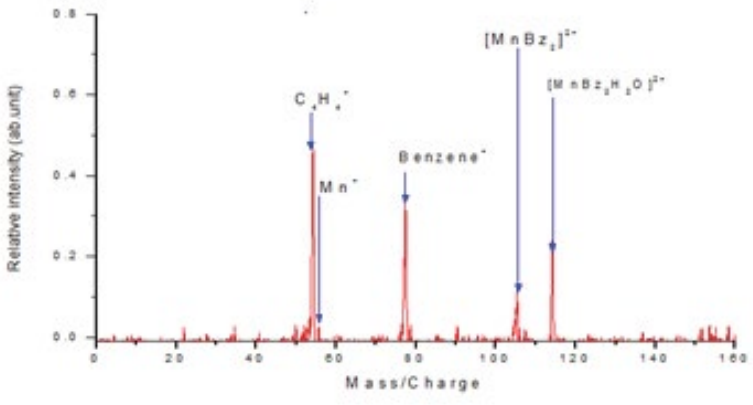

Figure 3: Photofragmentation mass spectrum of $[Mn(Benzene)_2]^{2+}$ (photon energy of 39760 cm^{-1}).

transfer followed by coulomb explosion between $[Mn(Benzene)]^+$ and $benzene^+$, the resulting momentum of Mn^+ could be too high to be quenched and confined by the buffer gas the resultant effect is that the $[Mn(Benzene)]^+$ ion was not successfully maintained in the trap before the detection process. Additional contributions to the photofragment spectrum could also come from $[Mn(Benzene)]^+$. If $[Mn(Benzene)]^+$ remain in the trap during each cycle it could dissociate to Mn and $Benzene^+$ as observed in the photo fragmentation mass spectrum at 55 and 79 amu for Mn^+ and $Benzene^+$ respectively. $Benzene^+$ eventually dissociating to C_2H_2 and $C_4H_4^+$ as in mechanism 1. The second possibility is that $[Mn(Benzene)_2]^{2+}$ loses a neutral benzene followed by a charge transfer process where the $[Mn(Benzene)]^{2+}$ dissociated to Mn^+ and $Benzene^+$. The peak at 55 amu in the mass spectra can be identified as Mn^+ if this is the case then subsequent photodissociation of $benzene^+$ could then produce $C_4H_4^+$ as in mechanism 2. $Benzene^+$ observed from the mass spectra could be a charge transfer product of either $[Mn(Benzene)_2]^{2+}$ or $[Mn(Benzene)]^{2+}$, or a photodissociation product from $[Mn(Benzene)]^+$. Hence the two proposed mechanism are possible and both could be thermodynamically feasible.

Figure 4 revealed four additional manganese-benzene monovalent photofragments of the complex ions when methane was introduced into the ion trap. They were dimethane metal complex ion $[Mn(Benzene)(CH_4)_2]^+$ at 165 amu, the carbonated ion $[Mn(Benzene)(CO_2)]^+$ at 177 amu, the hydrated dimethane complex ion $[Mn(Benzene)(CH_4)_2H_2O]^+$ at 183 amu and carbonated dimethyl complex ion $[Mn(Benzene)(CO_2)(CH_3)_2]^+$ at 207 amu. The photofragmentation route observed was the loss of $benzene^+$. Although $[Mn(Benzene)]^+$ was not observed in the photofragmentation mass spectrum of $[Mn(Benzene)_2]^{2+}$ (**Figure 3**) its appearance in the methane activation could probably be due to increase in its molecular mass as it coordinates with CH_4, H_2O and CO_2. This may have reduced the kinetic energy, stabilising and prolonging its life span, thereby enabling it to be trapped. A ground state calculation of the binding energy of methane with manganese Benzene complex dications ion were carried out at zero point energy, corrected at 298 K using Gaussian 09 with BVP86 and TPSSh with 6-311G++(d, p) basis sets (Table 1).

Two optimised geometries were observed, namely the C_{2V} eclipse (**Figure 5**) and C_2 staggered (**Figure 6**). In both cases of the C_{2V} and C_2 optimised structures the rings of the sandwich complex were not parallel but bent hemi-directed geometries, with a centroid-Mn-centroid angle of 180 distorted to approximately 171°. While the two benzene molecules were approximately equidistance from the manganese atom at 2.10 Å. The optimised structure of $[Mn(Benzene)]^{2+}$ gave bond length between manganese atom and the centre of benzene to be 1.60 Å and the manganese atom approximately equidistance from the six carbon atoms in benzene at 2.20 Å (**Figure 7**). At the optimised structure of $[Mn(Benzene)]^+$ the bond length between manganese atom and the centre of benzene to 1.50 Å and the manganese atom approximately equidistance from the six carbon atoms in benzene at 2.10 Å , (**Figure 8**). At the optimised geometry of $[Mn(Benzene)_2CH_4]^{2+}$ the initial centroid-Mn-centroid bond angle of 180° was distorted to 175.96° (**Figure 9**) while the initial hydrogen-carbon-hydrogen bond angles in methane also experienced distortion from 109.5° to between 108.81° to 115.14°. The manganese methane (Mn-C) distance from the optimised geometry was 2.0 Å and the distances between the benzene rings and the manganese were 1.70 and 1.80 Å respectively for the top and the down benzene molecules.

Figure 10 represents a one dimensional potential energy (PEC) curve model of $[Mn(Benzene)_2(CH_4)]^{2+}$ which explained the observed charge separation reaction qualitatively. The positions of these curves were determined by the

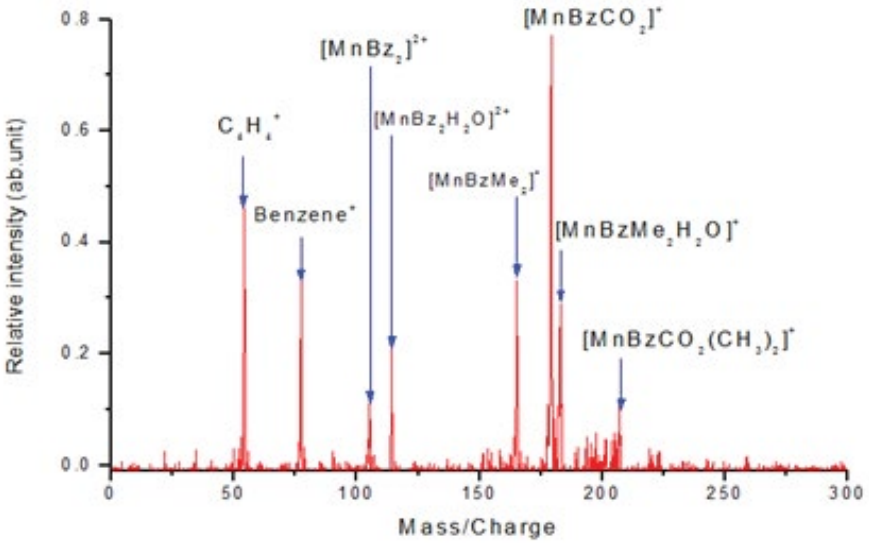

Figure 4: Photofragmentation mass spectrum of $[Mn(Benzene)_2]^{2+}$ with methane (Photon energy of 39760 cm^{-1}).

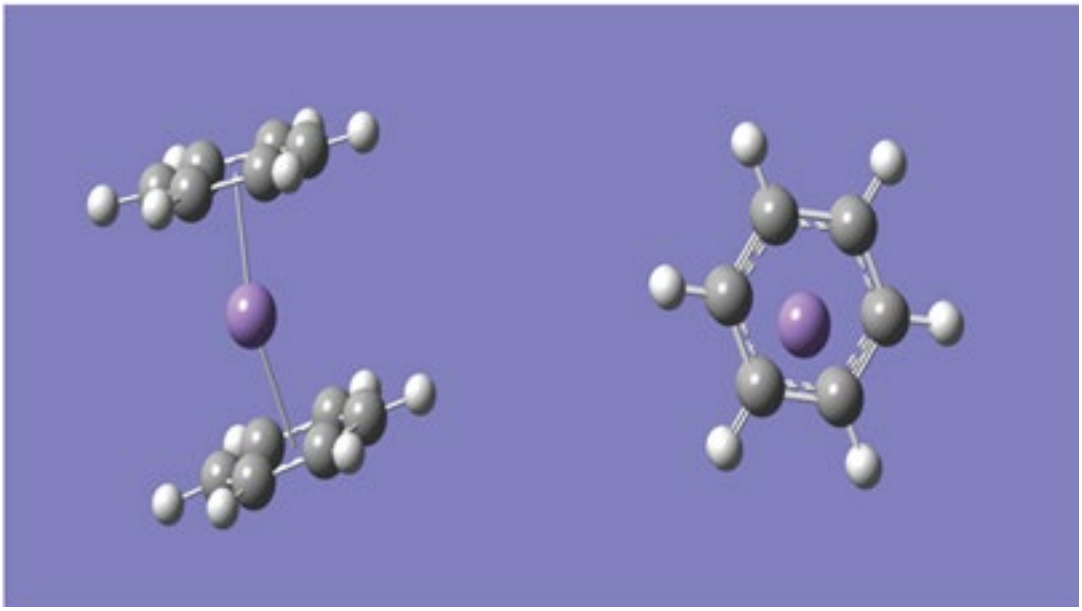

Figure 5: The optimized C_{2v} Eclipsed geometry using BVP86, 6-311++G(d,p) basic set.

exothermicity of the reactions they correspond to at infinite separation. From the curves, it was observed that the photo induced charge transfer to give $[Mn(Benzene)_2]^+$ and CH_4^+ from $[Mn(Benzene)_2CH_4]^{2+}$ was not observed because this reaction was endothermic as evidenced by observing the repulsive curve (green) lies above the attractive curve (black). At the optimised structure of $[Mn\ (Benzene)_2CH_4]^{2+}$ the manganese-carbon (Mn-C) distance of 2.0 Å corresponds to approximately 0.213 eV (20.55 kJ/mol) as the calculated binding energy from the PEC. At the optimised geometry the symmetry observed was C_1 for the $[Mn\ (Benzene)_2CH_4]^{2+}$ complex ion. The DFT calculated binding energy of methane to manganese benzene dication complex ion $[Mn(Benzene)_2]^{2+}$ at BP86/6- 311^{++}G(d, p) was 15.30 kJ/mol comparing with the calculated 20.55 kJ/mol recorded on the PEC. The difference of about 5.25 kJ/mol results from the fact that the calculated charge on the manganese metal centre at the optimised geometry of $[Mn(Benzene)_2CH_4]^{2+}$ was considerably reduced to 1.30 while a charge of Mn=2.0 was assumed in the PEC calculation.

Figure 11 demonstrated the ability of the coordinately unsaturated $[Mn(Benzene)]^+$ complex ion to accommodate a molecule of carbon dioxide in its vacant site to form the carbonated complex ion, $[Mn(Benzene)CO_2]^+$. At the optimised structure of Mn $(Benzene)CO_2]^+$ the oxygen atom (in the carbon dioxide) is coordinated with Mn ion from opposite side of the benzene ring. The linear geometry of carbon dioxide of 180° is slightly distorted to 179.05° and

Reaction	STRUCTURE	BVP86/kJ/mol	TPSSh/kJ/mol
$[MnBz_2]^{2+} \rightarrow Mn^{2+} + 2Bz$	C2v: Eclipsed	1140.04	1140.04
	C2: Staggered	1140.10	1140.1
$[Mn\ Bz_2]^{2+} \rightarrow [MnBz]^{+} + Bz^{+}$	C_{2v}: Eclipsed	250.10	250.10
	C_2: Staggered	250.10	250.10
$[Mn\ Bz_2]^{2+\rightarrow}\ [MnBz]^{2+} + Bz$	C2v: Eclipsed	305.14	305.10
	C2: Staggered	305.14	305.14
$[MnBz_2Me]^{2+} \rightarrow [MnBz_2]^{2+}\ + Me$		15.30	15.30
$[MnBzMe_2]^{+} \rightarrow [MnBz]^{+}\ + 2Me$		125.24	125.24
$MnBzMe_2]^{+} \rightarrow [MnBzMe]^{+}\ + Me$		51.77	51.75
$[MnBzCO_2]^{+} \rightarrow [MnBz]^{+} +\ CO_2$		76.40	76.40
$[MnBzMeH_2O]^{+} \rightarrow [MnBzH_2O]^{+} + Me$		19.75	19.75
$[MnBzMe_2H_2O]^{+} \rightarrow [MnBzH_2O]^{+} + 2Me$		48.33	48.33
$MnBzMe2H_2O]^{+} \rightarrow [MnBzMeH_2O]^{+} + Me$		28.59	28.60
$[MnBzH_2O]^{+} \rightarrow [MnBz]^{+} + H_2O$		302.78	302.78
$MnBzMe_2H2O]^{+} \rightarrow [MnBzMe_2]^{+} + H_2O$		225.88	225.88
$[MnBzCO_2(CH_3)_2]^{+} \rightarrow [MnBzCO_2CH_3]^{+} +\ CH_3$		108.75	108.75
$[MnBzCO_2CH_3]+ \rightarrow [MnBz]^{+} + CO^2 + CH_3$		272.05	272.05
$[MnBzCO_2(CH_3)_2]^{+} \rightarrow [MnBzCO_2]^{+} +\ 2CH_3$		304.4	304.40
$[MnBzCO_2(CH_3)^2]+ \rightarrow [MnBz]^{+} + CO_2 + 2CH_3$		380.80	380.80
$[MnBz(CH_3)_2]+ \rightarrow [MnBz]+\ + 2CH_3$		252.68	252.68
$[MnBzCO_2(CH_3)_2]^{+} \rightarrow [MnBz(CH_3)_2]^{+} + CO_2$		128.12	128.12

Table 1: Binding Energies for the Mn^{2+} Complexes with respect to various products formed and calculated using both BVP86/6311++G(d, p) and TPSSh/6311++G(d, p)

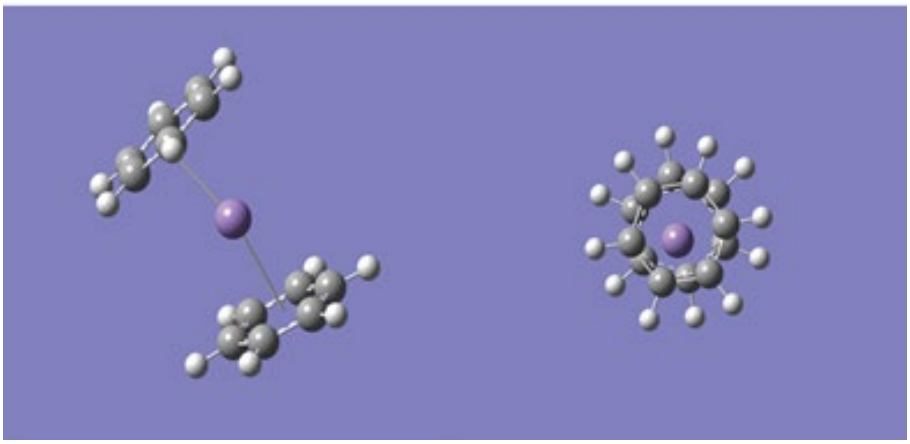

Figure 6: The optimized C_2 staggered geometry using BVP86, 6-311++G(d,p) basic set.

the shortest manganese oxygen (Mn-O) distance is 2.04 Å. All the calculated optimised geometries of $[Mn(Benzene)]^+$ with small molecules were done using BVP86 with 6-311^{++}G(d,p) basic set.

Figure 12 detailed the ability of the daughter photofragment $[Mn(Benzene)]^+$to form $[Mn(Benzene)(CH_3)_2]^+$ when methane was introduced into the ion trap. At the optimised structure the two methyl groups were arranged on the same surface and the carbon atoms (in the methyl groups) are coordinated with Mn ion from the opposite side of the benzene ring. The two manganese carbon (Mn-C) distances were equidistance at 2.04 Å. On the other hand, the ability of the $[Mn(Benzene)]^+$ to attract two molecules of methane to the coordinately unsaturated site to form dimethane

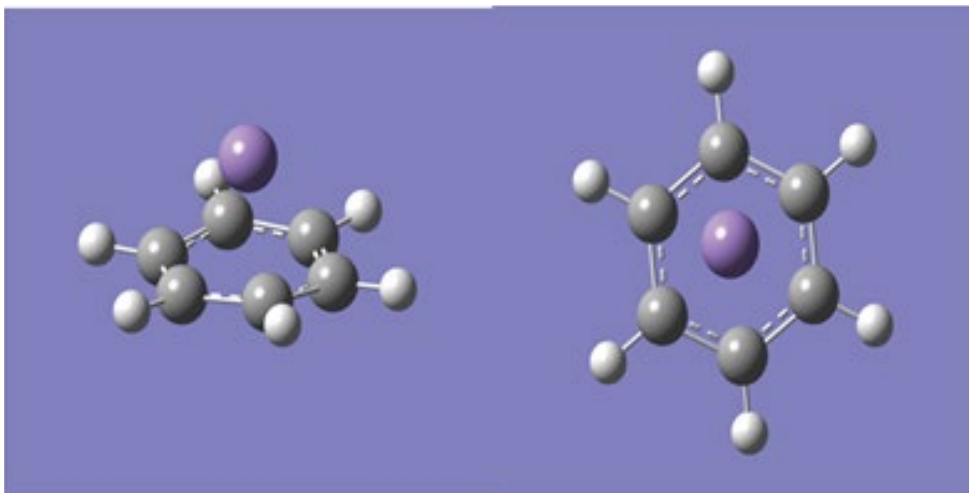

Figure 7: The optimized $[Mn(Benzene)]^{2+}$ geometry using BVP86, 6-311++G(d,p) basic set.

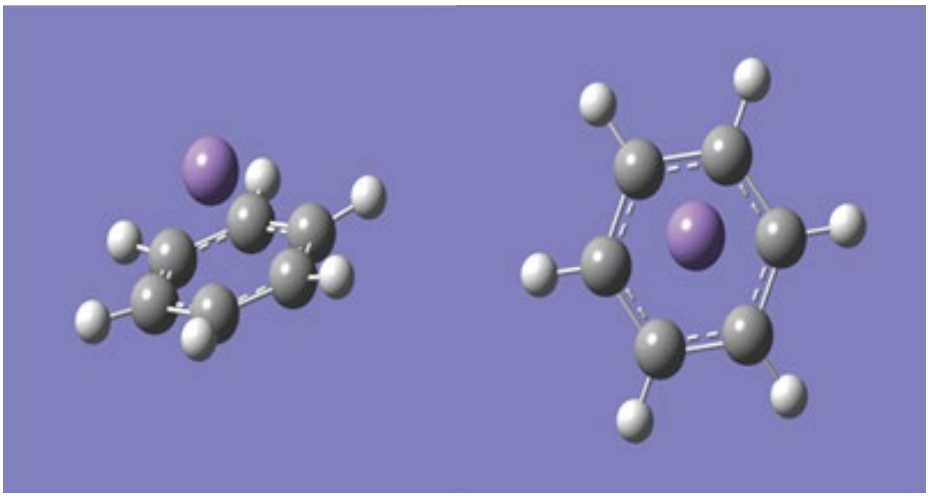

Figure 8: The optimized $[Mn(Benzene)]^{+}$ geometry using BVP86, 6-311++G(d, p) basic set.

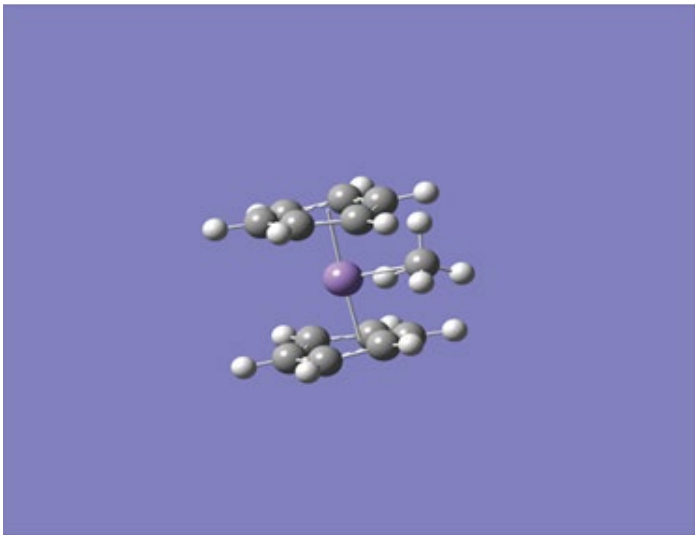

Figure 9: The optimized C_1 geometry of $Mn(Benzene)_2CH_4]^{2+}$ using BVP86, 6-311++G(d , p) basic set.

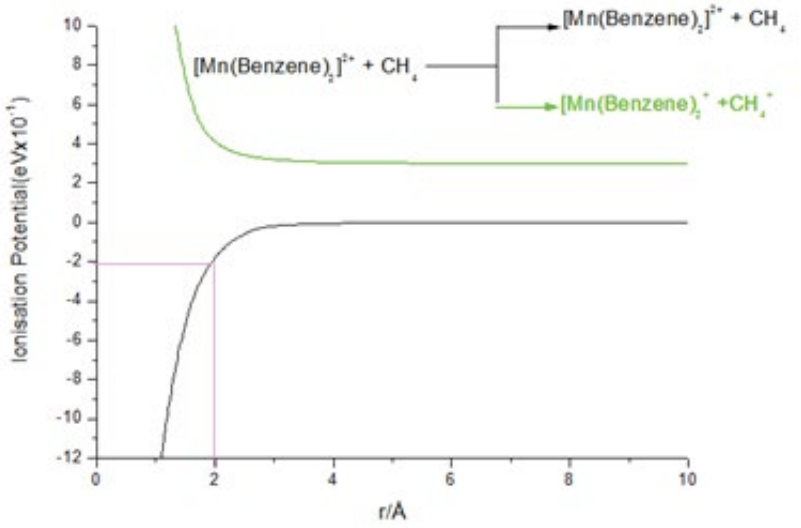

Figure 10: The potential energy surface curve model showing attractive curve of ion-ligand and repulsive curve.

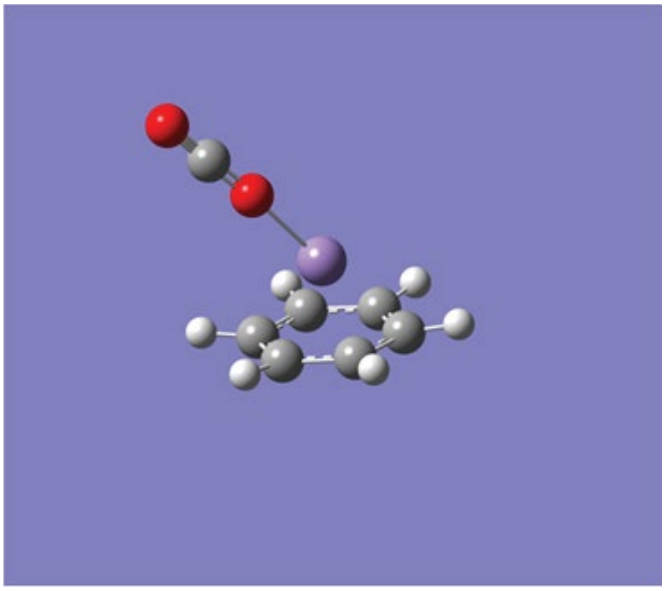

Figure 11: The optimised C_1 geometry of $[Mn(Benzene)CO_2]^+$ using BVP86, 6-311++G(d,p) basic set.

manganese mono benzene mono cation complex ion $[Mn(Benzene)(CH_4)_2]^+$ (**Figure 13**). The two methane molecules were arranged in the same surface and the carbon atoms (in the methane structure) were coordinated with Mn ion from the opposite side of the benzene ring. The two manganese carbon (Mn-C) distances were equidistance at 2.28 Å and the two methane molecules experienced similar distortion in angles between 105.52° and 116.33° at the optimised geometry.

At the optimised structure of $Mn(Benzene)CO_2(CH_3)]^+$ (**Figure 14**) the carbon dioxide and methyl molecules were arranged in the same surface and the oxygen atom (in the carbon dioxide) and the carbon atom (in the methyl group) were coordinated with Mn ion from the opposite side of the benzene ring. The linear geometry of carbon dioxide of 180° was distorted to 179.08° and the manganese oxygen (Mn-O) distance was 1. 94 Å while the manganese carbon (Mn-C) distance was 2.10 Å.

Furthermore, **Figure 15** demonstrated the possibility of the daughter photofragment complex ion $[Mn(Benzene)]^+$ to coordinate with two molecules of the methyl group in addition to the carbon dioxide. The three distinct small molecules are arranged in the same surface and the oxygen atom (in the carbon dioxide) and the carbon atoms (in the

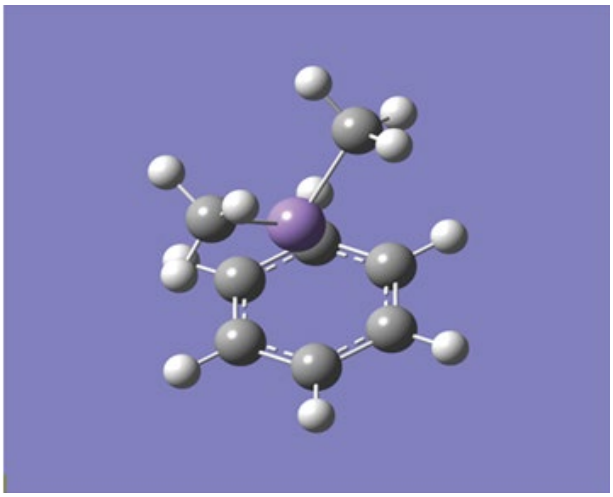

Figure 12: The optimized C_1 geometry of $[Mn(Benzene)(CH_3)_2]^+$ using BVP86, 6-311++G(d , p) basic set.

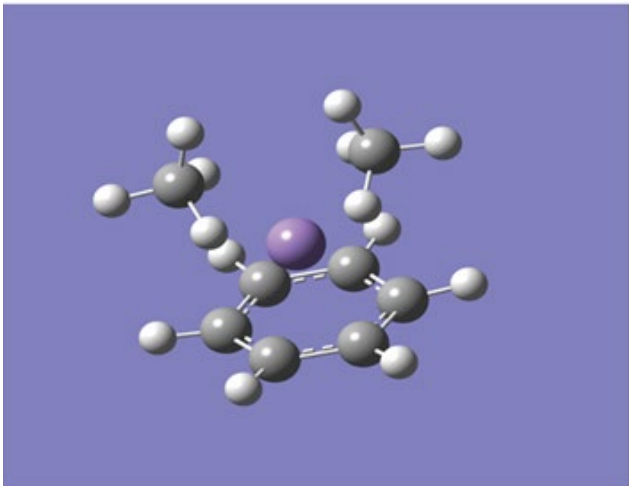

Figure 13: The optimized C_1 geometry of $[Mn(Benzene)\ (CH_4)_2\ ]^+$ using BVP86, 6-311++G(d,p) basic set.

methyl molecules) are coordinated with Mn ion from opposite side of the benzene ring. The linear geometry of carbon dioxide of 180^o was drastically distorted to 151.42^o and the manganese oxygen (Mn-O) shortest distance is 1.93 Å while the manganese carbon (Mn-C) distances were equidistance to 2.03 Å. The potentials in the $[Mn(Benzene)]^+$ complex ion to accommodate two molecules of methane alongside a molecule of water was recorded in **Figure 16**.

The three small molecules were arranged in the same surface and the oxygen atom (in the water) and the carbon atoms (in the methane molecules) were coordinated with Mn ion from opposite direction of the benzene ring as usual. The attractive feature observed with this geometry was the elongation of the manganese water distance in the initial none optimised geometry to double the distance in the optimised geometry resulting in the manganese oxygen (Mn–O) distance equating approximately to 4.90 Å while at the same time the oxygen hydrogen oxygen bond in water is distorted from 109.5^o to 104.04^0 in the optimised geometry. Like in the dimethyl, the manganese carbon (Mn–C) distances are equidistance at 2.03 Å.

CONCLUSION

The UV photofragmentation mass spectrum of the dication sandwich complex $[Mn(Benzene)_2]^{2+}$ has been recorded in the gas phase using a quadrupole ion trap mass spectrometer and Mn+, Benzene+, $[Mn(Benzene)_2H_2O)]^{2+}$, and $C_4H_4^+$ were observed as photofragments. The ground state DFT calculations identified optimized C_2 staggered and C_{2v} eclipsed conformers of $[Mn(Benzene)_2]^{2+}$. At optimised geometry the parallel sandwich complex were bent hemi-directed geometries, with a centroid-Mn-centroid angle of 180° distorted and the symmetry changed to C_s. Methane activation resulted in the formation of products $[Mn(Benzene)_2(CH_4)_2]^+$, $[Mn(Benzene)_2(CH_4)2H_2O)]^+$ and $[Mn(Benzene)_2CO_2(CH_3)^2]^+$. At the optimised geometry all the initial angles in the small molecules were observed to

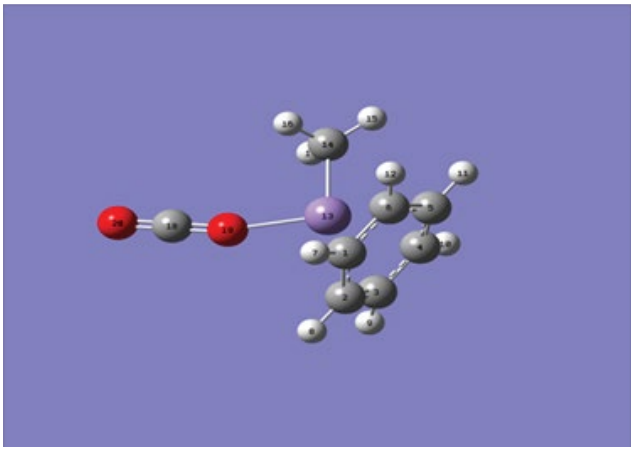

Figure 14: The optimized C_1 geometry of $[Mn(Benzene)CO_2(CH_3)]^+$ using BVP86/6-311++G(d,p) basic set.

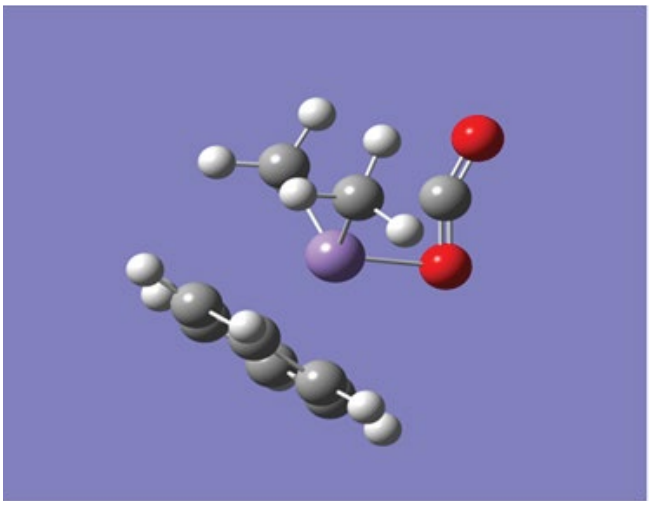

Figure 15: The optimized C_1 geometry of $[Mn(Benzene)CO_2(CH_3)_2]^+$ using BVP86, 6-311++G(d , p) basic set.

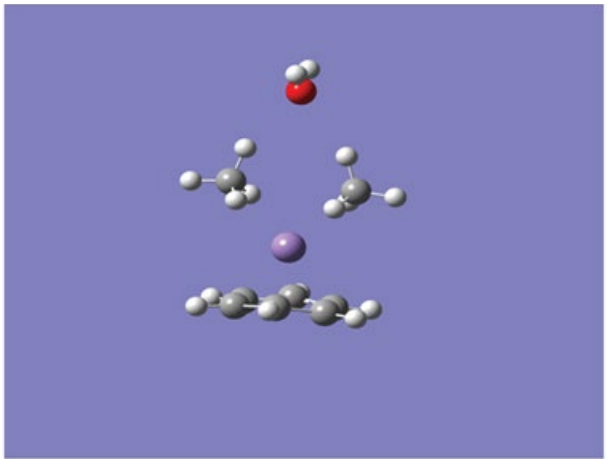

Figure 16: The optimized C_1 geometry of $[Mn(Benzene)H_2O(CH_4)_2]^+$ using BVP86, 6-311++G(d , p) basic set.

be distorted.

However, the calculated binding energy of methane to manganese complex ion on the PEC model was over estimated by 34% as compared to DFT calculation.

ACKNOWLEDGEMENT

The author would like to thank Professor Anthony Stace of University of Nottingham School of Chemistry, UK for all the sacrifice and support to see this research through, Dr Lifu Ma of University of Nottingham School of Chemistry for his contributions Prof Hazel Cox of the University of Sussex UK, Computational chemistry Department for the Software and computer time and the British government for awarding me 'International Excellence Research Award' which made the financial assistance for the program of experimental work in the Nottingham University possible.

REFERENCES

1. Soteras I, Orozco M, Luque F (**2008**) Induction effects in metal cation-benzene complexes. *J Phys Chem Chem Phys* 10: 2616-2624.
2. Kurikawa T, Hiroaki T, Masaaki H, Ken J, Tadashi A et al. (**1999**) Electronic properties of organometallic metal-benzene complexes [Mn(benzene)m (M = Sc-Cu)]. *Organometallics* 18: 1430-1438.
3. Xiang H, Yang J, Hou JG, Zhu Q (**2006**) One-dimensional transition metal-benzene sandwich polymers: Possible ideal conductors for spin transport. *J Am Chem Soc* 128: 2310-2314.
4. Martínez JI, García LJM, López MJ, Alonso JA (**2010**) Optical to ultraviolet spectra of sandwiches of benzene and transition metal atoms: Time dependent density functional theory and many-body calculations. *J Chem Phys* 132: 044314
5. Miyajima K, Yabushita S, Knickelbein MB, Nakajima A (**2004**) Ferromagnetism in one-dimensional vanadium−benzene sandwich clusters. *J Am Chem Soc* 126: 13202-13203.
6. Ravindra P, Bijan KR, Purusottam J, Miguel AB (**2001**) Electronic structure and properties of transition metal−benzene complexes. *J Am Chem Soc* 123: 3799-3808.
7. Miyajima K, Yabushita S, Knickelbein MB, Nakajima A (**2007**) Stern−Gerlach experiments of one-dimensional metal−benzene sandwich clusters: $M_n(C_6H_6)_m$ (M = Al, Sc, Ti, and V), J *Am Chem Soc* 129: 8473-848
8. Willey KF, Yeh CS, Robbins DL, Duncan MA (**1992**) Charge-transfer in the photodissociation of metal ion-benzene complexes. *J Phys Chem* 96: 9106-9111.
9. Meyer F, Farooq AK, Armentrout PB (**1995**) Thermochemistry of transition metal benzene complexes: Binding energies of $M(C_6H_6)x+$ (x = 1, 2) for M = Ti to Cu. *J Am Chem Soc* 117: 9740-9748.
10. Chia-NY, Klippenstein SJ (**1999**) Theory and modeling of the binding in cationic transition-metal−benzene complexes, *J Phys Chem A* 103: 1094-1103.
11. Hongming W, Taisuke O, Kiyoyuki T (**2009**) Revisiting magnetic coupling in transition-metal-benzene complexes with maximally localized Wannier functions *Phys Rev B* 79, 235118.
12. Jaeger TD, Duncan MA (**2005**) Vibrational spectroscopy of $Ni^+(benzene)_n$ complexes in the gas phase. *J Phys Chem A* 109: 3311-3317.
13. Jaeger TD, Deniz VH, Klippenstein SJ, Gert VH , Gerard M et al. (**2004**) Vibrational spectroscopy and density functional theory of transition-metal ion−benzene and dibenzene complexes in the gas phase. *J Am Chem Soc* 126: 10981-10991.
14. Tsuzuki S, Uchimaru T, Mikami M (**2003**). Is the cation/π interaction in alkaline-earth-metal dication/benzene complexes a covalent interaction? *J Phys Chem A* 107: 10414-10418.
15. Detlef S, Activation of Methane by Gaseous Metal Ions, Wiley Online Library.
16. Jean PL (**2001**) Methanol synthesis: A short review of technology improvements *Catal Today* 64: 3-8.
17. Hyman DG, Norman RH, Chandra BP (**1985**) The direct conversion of methane to methanol by controlled oxidation. *Chem Rev* 85:235-244.
18. Forster P et al. (**2007**) In climate change 2007: The physical science basis. contribution of working group i to the fourth assessment report of the intergovernmental panel on climate change, eds Solomon, S. et al.,Cambridge Univ. Press, UK.
19. Stace AJ (**2002**) Metal ion solvation in the gas phase: The quest for higher oxidation states. *J Phys Chem A* 106: 7993-8005.
20. Wu, G, Daniel C, Anthony JS (**2007**)Trapping and recording the collision-and photo-induced fragmentation

patterns of multiply charged metal complexes in the gas phase. *Int J Mass spectrom* 262: 211-219.

21. Kirschke S, Philippe B, Philippe C, Marielle S, Joseph GC et al. (**2013**) Three decades of global methane sources and sinks. *Nature Geosci* 6: 813-823.
22. Miyajima K, Nakajima A,Yabushita S, Knickelbein MB, Kaya K (**2004**) Ferromagnetism in One-Dimensional Vanadium−Benzene Sandwich Clusters *J Am Chem Soc* 126: 13202-13203.